Supporting Information

Heteroatom (Nitrogen/Sulfur)-Doped Graphene as an Efficient Electrocatalyst for Oxygen Reduction and Evolution Reactions

Jian Zhang [1], Jia Wang [2], Zexing Wu [2], Shuai Wang [2,*], Yumin Wu [1,*] and Xien Liu [2]

[1] College of Chemical Engineering, Qingdao University of Science & Technology, Qingdao 266042, P. R. China; jian8552@163.com (J.Z.)

[2] State Key Laboratory Base of Eco-chemical Engineering, College of Chemistry and Molecular Engineering, Qingdao University of Science & Technology, Qingdao 266042, P. R. China; wangjia3588@163.com (J.W.); splswzx@qust.edu.cn (Z.W.); liuxien@qust.edu.cn (X.L.)

* Correspondence: qustwangshuai@qust.edu.cn (S.W.); Tel.: +86-150-9202-5911; wuyumin001@126.com (Y.W.); Tel.: +86-138-5463-8500

Electrochemical Measurements in Alkaline Electrolyte

Firstly, 3.0 mg catalyst was adequately dispersed into the solution of ethanol (0.30 mL) and deionized water (0.15 mL) with the addition of 60.0 μL of Nafion solution (5.0 wt%), then a homogeneous ink was formed through vigorous ultrasonic. Whereafter, 5.0 μL of obtained catalyst ink (0.23 mg cm^{-2}) was dropped onto the working electrode surface for ORR, while 35.0 μL of the ink (0.21 mg cm^{-2}) was dropped onto Ni foam (1 × 1 cm) for OER. The coated electrode was dried with infrared radiation prior to use for ORR. The loading of 20% Pt/C was also 0.23 mg cm^{-2}.

OER activity measurements of the catalysts were evaluated by using a standard three-electrode electrochemical cell in 1 M KOH electrolyte. A reversible hydrogen electrode and carbon rod were used as reference electrode and counter electrode, respectively. All the LSV curves were obtained at a scanning rate of 10 mV s^{-1} within the potential range of 1.0–1.8 V (*vs* RHE).

Calculation of Electron Transfer Number (n) and % HO_2^- for Oxygen Reduction Reaction

On the basis of rotating disk electrode (RDE) measurements, the electron transfer numbers (n) per O_2 involved in ORR were calculated from the slopes of the Koutecky-Levich plots according to the following equations[1]:

$$\frac{1}{j} = \frac{1}{j_k} + \frac{1}{j_l} = \frac{1}{B\omega^{1/2}} + \frac{1}{j_k} \qquad (1)$$

where j is the measured current density, j_k and j_l are the kinetic and diffusion-limiting current densities, ω is the rotating rate of electrode (rpm). B is determined from the slope of the Koutecky-Levich plots according to the Levich equation.

$$B = 0.2nFC_{O_2}D_{O_2}^{2/3}\nu^{-1/6} \qquad (2)$$

where n is electron transfer number per oxygen molecule, F is Faraday constant (96,485 C mol^{-1}), C_{O2} is the bulk concentration of O_2 (1.2×10^{-6} mol cm^{-3}), υ is the kinetic viscosity of electrolyte (0.01 cm^2 S^{-1}). D_{O2} is the diffusion coefficient of O_2 in 0.1 M KOH and 0.1 M $HClO_4$ (1.9×10^{-5} cm^2 S^{-1}).

Hydrogen peroxide yields and the electron transfer number (n) were calculated by the following equations:

$$\%(HO_2^-) = 200 \times \frac{\frac{I_r}{N}}{I_d + \frac{I_r}{N}} \qquad (3)$$

$$n = 4 \times \frac{I_d}{I_d + \frac{I_r}{N}} \qquad (4)$$

where I_d is disk current, I_r is ring current, the collection efficiency (N) was determined to be 0.40 by using 10 mM $K_3[Fe(CN)_6]$.

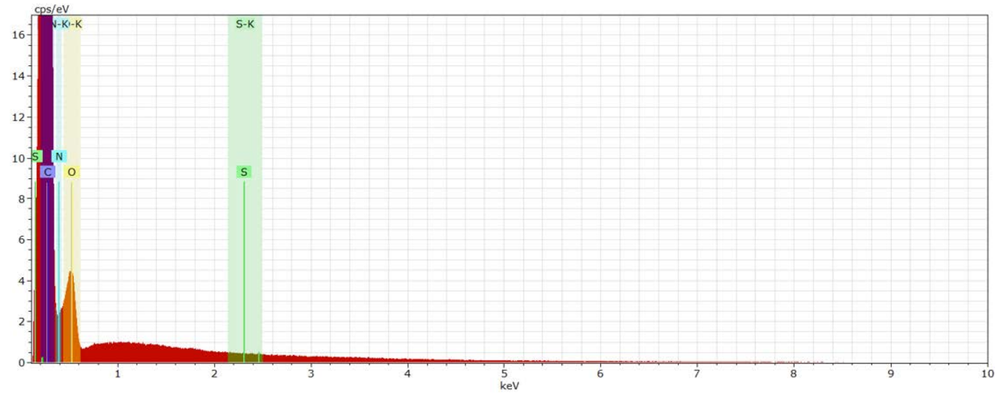

Figure S1. Energy dispersive spectrometer **(**EDS) of NSG.

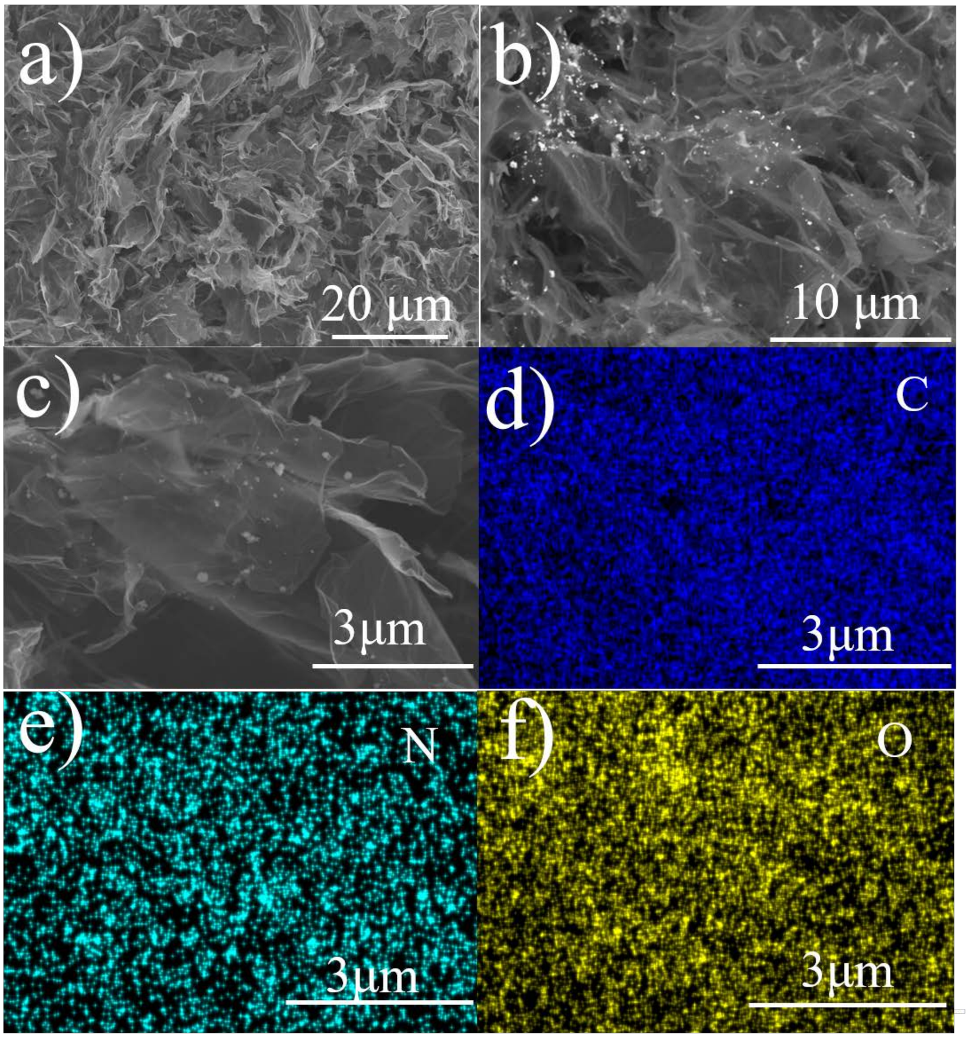

Figure S2. SEM (a-c) and mapping of C (d), N (e), O (f) of NG.

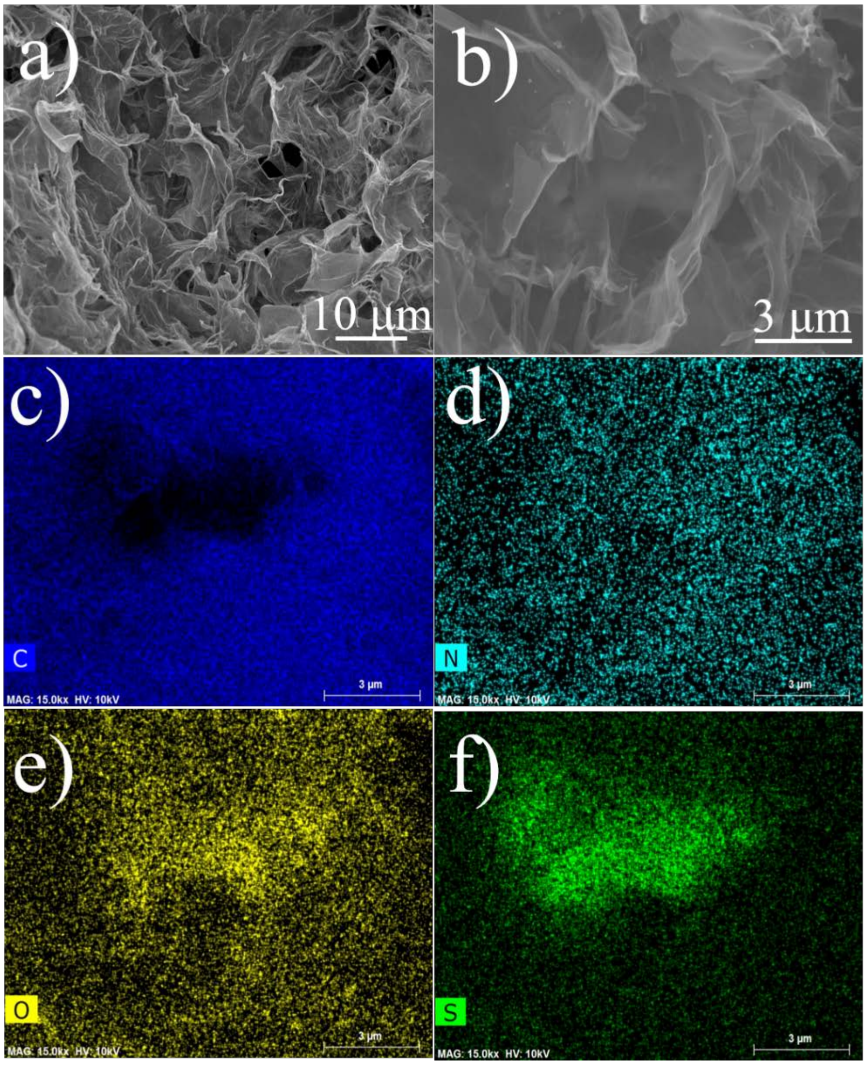

Figure S3. SEM (a, b) and mapping of C (c), N (d), O (e) and S (f) of SG.

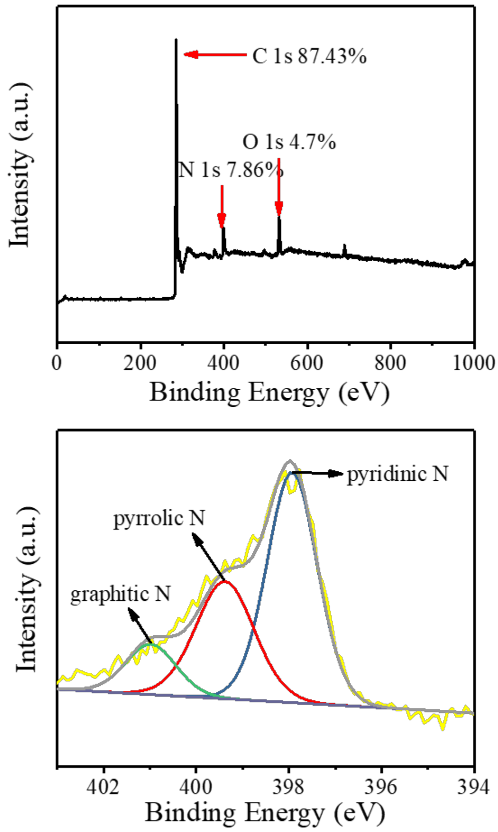

Figure S4. Full range XPS spectra of NG, XPS spectrum of C 1s and N 1s for NG.

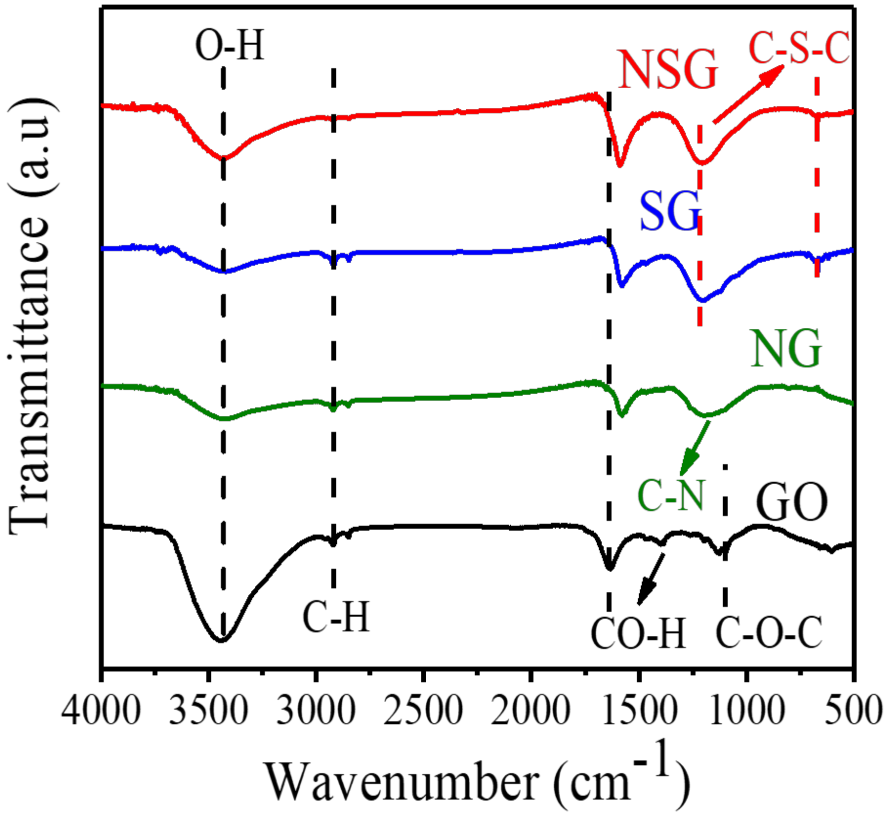

Figure S5. Fourier transform infrared spectroscopy (FTIR) of NSG, SG, NG and GO.

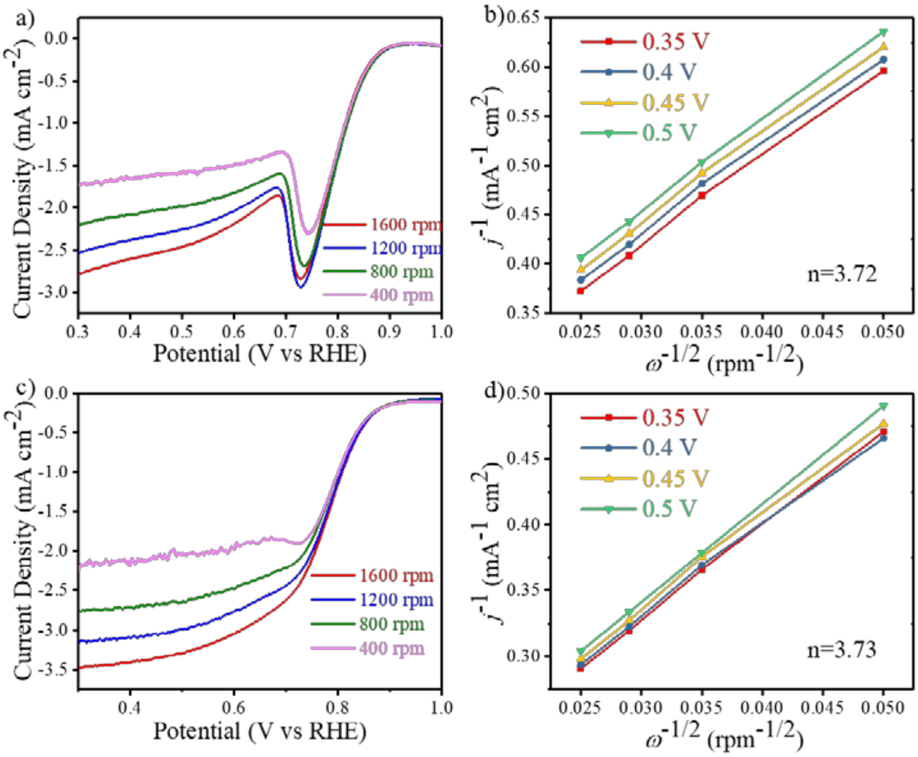

Figure S6. (**a**,**c**) Linear Scan Voltammetry (LSV) curves for SG and NG at different rotation rates in 0.1 M KOH. (**b**,**d**) Corresponding K-L plots at different potentials: 0.35, 0.4, 0.45, 0.5 V.

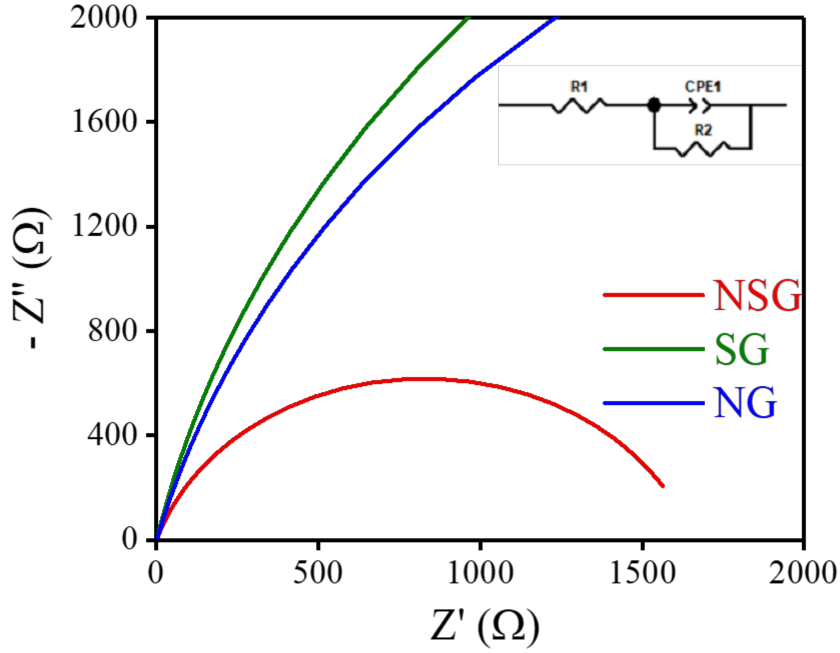

Figure S7. Nyquist plots of electrochemical impedance spectra (EIS) of NSG, SG and NG recorded in 1 M KOH. Inset: One-time-constant model equivalent circuit used for data fitting of EIS spectra

Table S1. Comparison of ORR and OER performance of NSG with the recently reported metal-free catalysts at 1600 rpm in KOH solution.

Catalysts	Loading (mg cm^{-2})	$E_{1/2}$ ORR Half-Wave Potential (V vs. RHE)	Onset Potentials (V vs. RHE)	$E_{j=10}$ OER@ 10 mA cm^{-2} (V vs. RHE)	References
NSG	0.23	0.84	0.95	1.62	This work
N, S-GCNT	0.23	0.79	0.93	1.61	[2]
N,P-carbon paper	0.20	0.67	0.94	1.63	[3]
N-graphene/CNT	0.2548	/	0.88	1.63	[4]
Ni–MnO/rGO	0.25	0.78	0.94	1.60	[5]
CMO/20N-rGO	0.12	0.79	0.93	1.68	[6]
Co-CoO/N-rGO	0.21	0.78	0.88	1.62	[7]
S-Co_9–xFe_xS_8@rGO	0.5	0.84	0.94	1.52	[8]
$Fe_{0.5}Co_{0.5}O_x$ /NrGO-300	0.5	0.82	0.91	1.487	[9]
$NiCo_2O_4$/RGO-1_RGO	/	0.77	0.90	1.631	[10]

Mark # RHE potentials conversion from the original potentials in the reference.

$V_{RHE} = V_{Ag/AgCl} + 0.059pH + 0.197$

References

1. Zhou, R.; Zheng, Y.; Jaroniec, M.; Qiao, S.-Z. Determination of the electron transfer number for the oxygen reduction reaction: From theory to experiment. *ACS Catal.* **2016**, *6*, 4720-4728.
2. Zhang, J.; Song, X.; Li, P.; Wu, Z.; Wu, Y.; Wang, S.; Liu, X. Sulfur, nitrogen co-doped nanocomposite of graphene and carbon nanotube as an efficient bifunctional electrocatalyst for oxygen reduction and evolution reactions. *J. Taiwan Inst. Chem. E.* **2018**, https://doi.org/10.1016/j.jtice.2018.07.040.
3. Ma, T.Y.; Ran, J.; Dai, S.; Jaroniec, M.; Qiao, S.Z. Phosphorus-doped graphitic carbon nitrides grown in situ on carbon-fiber paper: Flexible and reversible oxygen electrodes. *Angew. Chem. Int. Ed.* **2015**, *54*, 4646-4650.
4. Tian, G.L.; Zhao, M.Q.; Yu, D.; Kong, X.Y.; Huang, J.Q.; Zhang, Q.; Wei, F. Nitrogen-doped graphene/carbon nanotube hybrids: In situ formation on bifunctional catalysts and their superior electrocatalytic activity for oxygen evolution/reduction reaction. *Small* **2014**, *10*, 2251-2259.
5. Fu, G.; Yan, X.; Chen, Y.; Xu, L.; Sun, D.; Lee, J.M.; Tang, Y. Boosting bifunctional oxygen electrocatalysis with 3D graphene aerogel-supported Ni/MnO particles. *Adv. Mater.* **2018**, *30*.
6. He, X.; Yin, F.; Yuan, S.; Liu, N.; Huang, X. Hybrid spinel oxides/N-doped reduced graphene oxide as highly-active bifunctional electrocatalysts for oxygen reduction/evolution reactions. *Chem. Electro. Chem.* **2016**, *3*, 1107-1115.
7. Liu, X.; Liu, W.; Ko, M.; Park, M.; Kim, M.G.; Oh, P.; Chae, S.; Park, S.; Casimir, A.; Wu, G., *et al.* Metal (Ni, Co)-metal oxides/graphene nanocomposites as multifunctional electrocatalysts. *Adv. Funct. Mater.* **2015**, *25*, 5799-5808.
8. Liu, T.; Yang, F.; Cheng, G.; Luo, W. Reduced graphene oxide-wrapped $Co_{9-x}Fe_xS_8$/Co,Fe-N-C composite as bifunctional electrocatalyst for oxygen reduction and evolution. *Small* **2018**, *14*, 1703748.
9. Wei, L.; Karahan, H.E.; Zhai, S.; Liu, H.; Chen, X.; Zhou, Z.; Lei, Y.; Liu, Z.; Chen, Y. Amorphous bimetallic oxide-graphene hybrids as bifunctional oxygen electrocatalysts for rechargeable Zn-air batteries. *Adv. Mater.* **2017**, *29*, 1-10.
10. Kumar, K.; Loupias, L.; Canaff, C.; Morisset, S.; Pronier, S.; Morais, C.; Habrioux, A.; Napporn, T.W.; Kokoh, K.B. Preparation and electrochemical properties of $NiCo_2O_4$ nanospinels supported on graphene derivatives as earth-

abundant oxygen bifunctional catalysts. *Chem. Phys. Chem.* **2018**, *19*, 319-326.